Characterization of the solution properties and conformation of pneumolysin, the membrane-damaging toxin of *Streptococcus pneumoniae*

Peter J. MORGAN,*‖ Paul G. VARLEY,† Arthur J. ROWE,‡ Peter W. ANDREW* and Timothy J. MITCHELL§

*Department of Microbiology, University of Leicester, Leicester LE1 9HN, †Laboratory of Molecular Structure, National Institute of Biological Standards and Control, Blanche Lane, South Mimms, Potters Bar, Herts EN6 3QG, ‡NCMH, Department of Biochemistry, University of Leicester, Leicester LE1 9HN, and §Department of Immunology, Leicester Royal Infirmary, Leicester LE1 5WW, U.K.

Pneumolysin is a membrane-damaging toxin produced by *Streptococcus pneumoniae*. In order to understand fully the mode of action of this toxin, it is necessary to have an appreciation of the size, self-association behaviour and solution conformation of pneumolysin. A combination of analytical ultracentrifugation methodologies has shown that pneumolysin lacks self-association behaviour in solution and has provided a weight-average $M_r(\bar{M}_w)$ of 52000 ± 2000, which was in agreement with that derived from the amino acid sequence. By determining a sedimentation coefficient $(s^0_{20,w})$ of 3.35 ± 0.10 S, it was possible to suggest a model for the gross solution conformation of pneumolysin monomers. Spectroscopic methods provide additional secondary and tertiary structure information.

INTRODUCTION

The membrane-damaging toxin pneumolysin is an important virulence factor for the bacterium *Streptococcus pneumoniae* (Berry et al., 1989). To understand fully the virulence of this major human pathogen, one must understand the mode of action of this toxin. Pneumolysin is one of a family of so-called 'thiol-activated cholesterol-inhibitable' toxins (Alouf and Geoffroy, 1991). These cytolytic toxins form pores in cholesterol-containing membranes. Given the wealth of structural information gathered to date (Mitchell et al., 1992), on pneumolysin, it can serve as a paradigm for this group of toxins. The current view concerning the mode of action of this family of toxins, until now based mainly on work with streptolysin O (Bhakdi et al., 1985), is that toxin monomers bind to target-cell membranes via cholesterol, insert into the lipid bilayer where they diffuse together and oligomerize to form pores.

During this process monomers may undergo a conformational change in moving from the hydrophilic environment of the fluid phase to the hydrophobic environment of the lipid bilayer. Possibly, further conformational changes occur during oligomer formation. To discern this process it is necessary to describe the behaviour of the toxin in each of the environments it encounters. A previous paper has described a method for expressing and purifying recombinant pneumolysin in large enough quantities for a detailed biophysical study (Mitchell et al., 1989). The present paper describes the characterization of the properties and conformation of pneumolysin in aqueous solution.

MATERIALS AND METHODS

Materials

All chemicals used were Analytical grade (Fisons) unless otherwise stated. All protein samples were dissolved in phosphate buffered saline (PBS): 8 mM Na_2HPO_4, 1.5 mM KH_2PO_4, 0.137 M NaCl, 2.5 mM KCl, pH 7.3.

Purification of recombinant wild-type pneumolysin

Wild-type pneumolysin protein was expressed in *Escherichia coli* JM109 and purified as described previously (Mitchell et al., 1989). Sample purity was checked by SDS/PAGE analysis and haemolytic activity assayed as described previously (Mitchell et al., 1989).

Analytical ultracentrifugation

Measurements were made using a Beckman Optima XL-A analytical ultracentrifuge. All samples were dialysed exhaustively against PBS. All solute distributions were recorded via their absorption at 278 nm. The low-speed sedimentation-equilibrium method was employed (Creeth and Pain, 1967). Multichannel, 'Yphantis-type' centrepieces (Yphantis, 1964) were used, enabling the simultaneous measurement of multiple samples. It was considered that equilibrium had been established when two consecutive scans, recorded several hours apart, were identical. The final solute distribution ASCII data were captured and analysed on the IBM 2084Q Phoenix mainframe at the University of Cambridge, using the FORTRAN MSTARA program (Harding et al., 1993). Whole-cell weight-average $M_r(\bar{M}_w)$ values were extracted by using the limiting value at the cell base (i.e. at $\xi = 1$, where ξ is the normalized radial displacement parameter) of the M^* function (Creeth and Harding, 1982). The partial specific volume $(\bar{v})$ was calculated from the known amino acid composition (Walker et al., 1987) by use of the additivity rule and values for the individual amino acid residues (Perkins, 1986). For sedimentation-velocity analysis, consecutive scans were recorded at regular intervals. Sedimentation coefficient $(s_{20,b})$ values were determined in the standard way (van Holde, 1985), by measuring the rate of movement of the boundary per unit centrifugal field and normalized to standard conditions (water as a solvent at 20.0 °C) before being plotted against concentration (which must be corrected for radial dilution). Extrapolation to infinite dilution yielded $s^0_{20,w}$.

C.d. and fluorescence measurements

C.d. spectra were measured using a Jasco J-720 spectropolarimeter. The spectra shown are an average of 16 scans with the average of 16 baseline scans subtracted. All spectra measured

in the near-u.v. (250–320 nm) region were of a protein solution in a 1.0 cm-pathlength cuvette, and in the far-u.v. (190–250 nm) region a 0.05 cm-pathlength cuvette was used. Molar ellipticities ($[\theta]$) were determined using an $A_{280}^{1\%}$ value of 13.6, calculated from the amino acid sequence (Walker et al., 1987). An M_r of 52800 (Walker et al., 1987) was used to calculate molar ellipticities. Secondary structure prediction was performed by comparing the data collected in the far-u.v. spectrum with the reference spectrum of each secondary structure element, according to the method of Yang et al. (1986).

The fluorescence spectra were measured with a Spex Fluoromax single-photon-counting spectrofluorimeter. The bandwidth was 4.25 nm on both the excitation and emission monochromators and the protein concentration adjusted to give an absorbance value at the excitation wavelength of approx. 0.05 in a 1.0 cm-pathlength cuvette. Spectra are an average of four scans with the equivalent baselines subtracted. All samples were clarified by centrifugation at 10000 rev./min ($r_{av.}$ 3.7 cm) for 10 min in a microcentrifuge prior to measurement.

RESULTS AND DISCUSSION

Previous studies (Mitchell et al., 1989) concluded that the recombinant and native pneumolysin are structurally and functionally equivalent. Evidence of this included N-terminal amino acid sequence, specific haemolytic activity, degree of inhibition by cholesterol and anti-pneumolysin antisera, as well as their effect on human complement and polymorphonuclear leucocytes.

Analytical ultracentrifugation

Sedimentation-equilibrium measurements enabled the determination of a whole-cell $\bar{M}_w$ of 52000 ($\pm$2000) (from the extrapolation of the M^* function to the cell base ($\xi = 1$); Figure 1a) which is in agreement with the sequence M_r of 52800. $\bar{M}_w$ represents the average M_r for the whole solute distribution, and the presence of large oligomers would have increased this value noticeably. Therefore it would seem that recombinant pneumolysin exists as a monomer, under the loading concentrations and buffer conditions described. Additionally, there are no detectable association phenomena, over a range of increasing concentrations (Figure 2), since the slight concomitant decrease in $\bar{M}_w$ seen can be wholly attributed to the effect of a second virial coefficient of a magnitude determined solely by the excluded volume of a particle of the axial ratio postulated ($= 15.8$ v/v, cf. 8 for a spherical particle); at neutral pH and in the presence of 137 mM neutral salt, charge contributions to the virial coefficient will be negligible (Wills and Winzor, 1992). The $\ln A$-versus-ξ plot (Figure 1b) was found to be linear, providing further evidence of protein homogeneity (see Creeth and Pain, 1967). It is therefore clear that oligomerization does not occur in solution, at least not to an extent detectable by the techniques used.

Sedimentation-velocity analysis showed a single symmetrical sedimenting boundary (Figure 3a). A slight elevation in the centrifugal region of the plateau region was noticed, but this was found to be constant from trace to trace throughout the run and hence was attributable to a small amount of background optical contamination rather than to any significant aggregation of the sample.

The regression of the sedimentation coefficient (s) on solute concentration (c) can be characterized by a linear coefficient, k_s, in the equation:

$$s = s^0(1 - k_s c)$$

where s^0 is the limiting value for the sedimentation coefficient. In the presence of significant self-association, the regression becomes positive and may show positive curvature (Gilbert and Gilbert, 1973). Fitting the present data set shows a simple linear negative regression. A value for k_s of 7.26 ml·g^{-1}, combined with the extrapolated value obtained for $s_{20,w}^0$ of 3.35 S and an assumed $\bar{V}_s/\bar{v}$ of 1.4 yields (where $\bar{V}_s$ is the swollen volume, Rowe, 1977) an estimate for the M_r of 55500. This latter value is not significantly different from that of the monomer, providing further strong evidence for the absence of significant self-association.

A combination of the absolute $\bar{M}_w$ and the sedimentation coefficient at infinite dilution yields an estimate (van Holde, 1985) for the frictional ratio of pneumolysin monomers (Table 1) corresponding to an axial ratio of between 5.3 and 8.6, whether calculated using a hydrated (assuming hydration $= 0.4$ g of water/g of protein) or anhydrous volume. The hydrodynamic properties of pneumolysin are summarized in Table 1. The
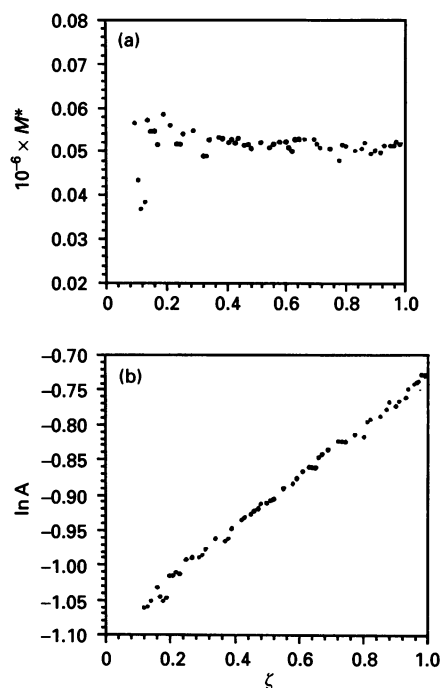
Figure 1 (a) Sedimentation equilibrium and (b) a plot of ln absorbance versus ξ

(a) Conditions: 10000 rev./min; 20.0 °C; loading concentration 0.5 mg/ml. Shown is a plot of the M^* function versus ξ (the normalized radial displacement parameter) for pneumolysin. $\xi = (r^2 - a^2)/(b^2 - a^2)$, where r is the radial displacement and a and b are the corresponding values at the meniscus and cell base respectively. (b) Run conditions were as in (a).
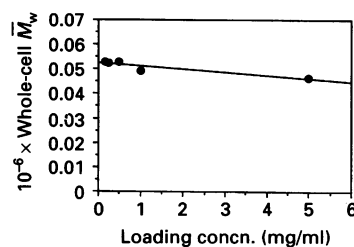
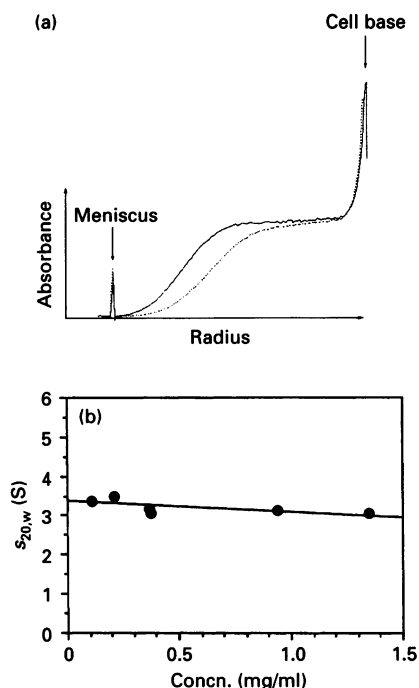**Figure 2 Plot of whole-cell $\bar{M}_w$ versus concentration**

Figure 3 **(a) Sedimentation-velocity profiles for pneumolysin and (b) plot of sedimentation coefficient versus concentration**

The loading concentration was 1.3 mg/ml, the rotor speed 40000 rev./min, the temperature 20.0 °C and the scan interval was 30 min. Sedimentation is from left to right. (b) Run conditions were as in (a).

Table 1 Hydrodynamic properties of pneumolysin

$\bar{v}$ was calculated from the amino acid sequence as described in the Materials and methods section. $\bar{M}_w$ was determined from Figure 1(a) by extrapolating the M^* function to $\xi = 0$ (i.e. the cell base). $s^0_{20,w}$ was determined as described in the Materials and methods section. An estimate of the hydration was calculated from the amino acid composition (see Table 2) using the method of Kuntz (1971) based on the hydration of individual amino acid residues. The frictional ratios (f/f_0) were calculated from the frictional coefficient (f_0) values derived for anhydrous spheres or hydrated spheres and the experimentally measured value (f).

Parameter	Value
Partial specific volume $\bar{v}$ (ml/g)	0.737
$\bar{M}_w$	52000 ± 2000
$s^0_{20,w}$ (S)	3.35 ± 0.10
k_s (ml/g)	7.26
Hydration (g of water/g of protein)	0.40
Frictional coefficient (f) (experimentally determined) (g/s)	6.88×10^{-8}
Frictional coefficient (f_0) (g/s)	
Anhydrous sphere	4.69×10^{-8}
Hydrated sphere	5.42×10^{-8}
Frictional ratio (f/f_0)	
Anhydrous sphere	1.47
Hydrated sphere	1.27

analytical-ultracentrifuge data obtained are consistent with the proposed mechanism of toxin pore formation (Bhakdi et al., 1985) in which water-soluble monomers insert into target membranes before oligomerization. However, it is still unclear whether
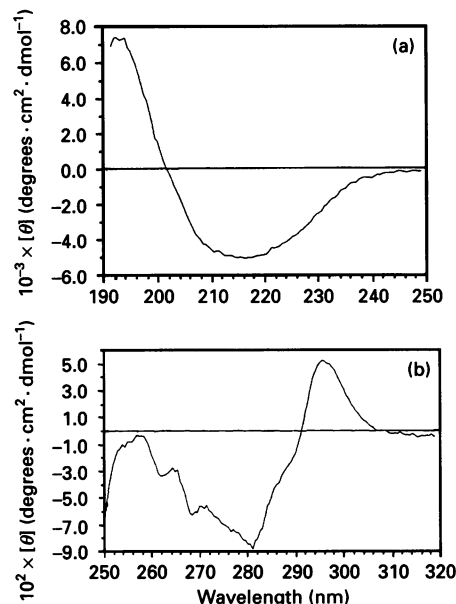

Figure 4   Far- (a) and near (b)-u.v. c.d. spectra of pneumolysin

(a) The spectrum is the average of 16 scans with the baseline subtracted. The protein concentration was 0.4 mg/ml. Ellipticities are expressed per mol of peptide bond. Spectra were recorded using a 0.05 cm-pathlength cell. (b) The spectrum is the average of 16 scans with the baseline subtracted. The protein concentration was 0.8 mg/ml. Ellipticities are expressed per mol of protein. Spectra were recorded using a 1.0 cm-pathlength cell.

Table 2   Amino acid composition of pneumolysin derived from the DNA sequence (Walker et al., 1987)

Amino acid	No. of residues	Amino acid	No. of residues
Asp	36	Val	45
Asn	25	Met	6
Glu	30	Ile	23
Gln	22	Leu	41
Pro	17	Tyr	19
Thr	36	Phe	14
Ser	35	His	8
Gly	26	Lys	30
Ala	29	Arg	20
Cys	1	Trp	8

the oligomerization occurs at the surface of the membrane following binding to a receptor (i.e. cholesterol) or after insertion of monomers into the membrane, followed by their lateral diffusion and subsequent oligomerization to become a functional pore.

Secondary-structure analyses

The far-u.v. c.d. spectrum for pneumolysin is shown in Figure 4(a). Estimation of the secondary-structure content gave similar amounts of α-helix (31 %), β-sheet (36 %), random coil (28 %) and 5 % β-turn. Secondary-structure prediction (Devereux et al., 1984) based on the amino acid sequence yielded no convincing information. The near-u.v. spectrum, shown in Figure 4(b), has a major negative peak centred at about 280 nm and is typical of
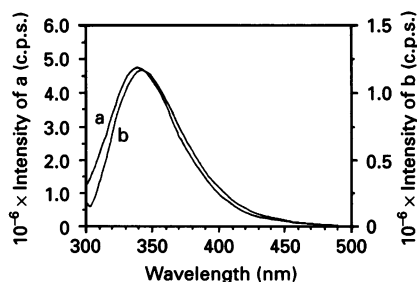
Figure 5 Fluorescence spectra of pneumolysin, with excitation wavelengths of (a) 280 nm and (b) 295 nm

Spectra were recorded using a 1.0 cm-pathlength cell; the loading concentration was 0.04 mg/ml.

a folded protein. There is also a positive peak at 295 nm representative of the tryptophan element within pneumolysin (Strickland, 1974). As a consequence of the number of aromatic groups found in pneumolysin (see Table 2), it is not possible to attribute peaks to individual aromatic groups. However, measuring the near-u.v. spectrum of pneumolysin can provide a highly sensitive fingerprint for the conformation of the fully active toxin in solution. Given the strong possibility that pneumolysin will form part of a new vaccine (Mitchell et al., 1992), such a fingerprint forms an ideal baseline measurement for subsequent control of vaccine quality.

The fluorescence spectra of pneumolysin at excitation wavelengths of 280 nm and 295 nm are shown in Figures 5(a) and 5(b) respectively. The emission maxima of the spectra are 340 nm and 342 nm for the excitation wavelengths of 280 nm and 295 nm respectively. The spectra are typical of proteins containing multiple tryptophan residues. Pneumolysin has eight tryptophan residues (see Table 2). The location of the maximum at 342 nm after excitation at 295 nm suggests that the majority of the tryptophan side chains are at least partially exposed to solvent (Lakowitz, 1983).

If the tryptophan residues are exposed to solvent, they will be available to interact with other molecules. Pneumolysin has an 11-amino-acid region which is conserved within this toxin family and is known to be functionally important (Mitchell et al., 1992).

This region contains three tryptophan residues with an intervening glutamate residue. It has been suggested that these tryptophans play a role in toxin function by interaction with cholesterol, in a fashion analogous to the tryptophans in gramicidin A (de Kruijff, 1990).

The characterization of wild-type pneumolysin as described will serve as a baseline for further investigations. A similar approach will be used to study a series of mutant pneumolysins produced by site-directed mutagenesis, whose biological properties have already been reported (Mitchell et al., 1992), to investigate the process of oligomerization in pneumolysin.

REFERENCES

Alouf, J. E. and Geoffroy, C. (1991) in Sourcebook of Bacterial Toxins (Alouf, J. E. and Freer, J. H., eds.), pp. 147–186, Academic Press, London

Berry, A. M., Yother, J., Briles, D. E., Hansman, D. and Paton, J. C. (1989) Infect. Immun. **57**, 2037–2042

Bhakdi, S., Tranum-Jensen, J., Sziegoleit, A. (1985) Infect. Immun. **47**, 52–60

Creeth, J. M. and Pain, R. H. (1967) Progr. Biophys. Mol. Biol. **17**, 217–287

Creeth, J. M. and Harding, S. E. (1982) J. Biochem. Biophys. Methods **7**, 25–34

de Kruijff, B. (1990) Biosci. Rep. **10**, 127–130

Devereux, J., Haeberli, P. and Smithies, O. (1984) Nucleic Acids Res. **12**, 387–395

Gilbert, L. M. and Gilbert, G. A. (1973) Methods Enzymol. **27D**, 273–296

Harding, S. E., Horton, J. C. and Morgan, P. J. (1993) Analytical Ultracentrifugation in Biochemistry and Polymer Science (Harding, S. E., Horton, J. C. and Rowe, A. J., eds.), pp. 275–294, Royal Society of Chemistry, Cambridge

Kuntz, I. D. (1971) J. Am. Chem. Soc. **93**, 514–516

Lakowitz, J. R. (1983) in Principles of Fluorescence Spectroscopy (Lakowitz, J. R., ed.), Plenum Press, New York

Mitchell, T. J., Walker, J. A., Saunders, F. K., Andrew, P. W. and Boulnois, G. J. (1989) Biochem. Biophys. Acta **1007**, 67–72

Mitchell, T. J., Andrew, P. W., Boulnois, G. J., Lee, C. J., Lock, R. A. and Paton, J. C. (1992) in Bacterial Protein Toxins (Witholt, B., Alouf, J. E. and Boulnois, G. J., eds.), pp. 429–438, Gustav Fischer, Stuttgart

Perkins, S. J. (1986) Eur. J. Biochem. **157**, 169–180

Rowe, A. J. (1977) Biopolymers **16**, 2595–2610

Strickland, E. H. (1974) CRC Crit. Rev. Biochem. **2**, 113–175

van Holde, K. E. (1985) Physical Biochemistry, 2nd edn., Prentice-Hale Englewood Cliffs, NJ

Walker, J. A., Allen, R. L., Falmagne, P., Johnson, M. K. and Boulnois, G. K. (1987) Infect. Immun. **55**, 1184–1189

Wills, P. R. and Winzor, D. J. (1993) in Analytical Ultracentrifugation in Biochemistry and Polymer Science (Harding, S. E., Horton, J. C. and Rowe, A. J., eds.), pp. 311–330, Royal Society of Chemistry, Cambridge

Yang, J. T., Wu, C. S. C. and Martinez, H. M. (1986) Methods Enzymol. **130**, 208–269

Yphantis, D. A. (1964) Biochemistry **3**, 297–317